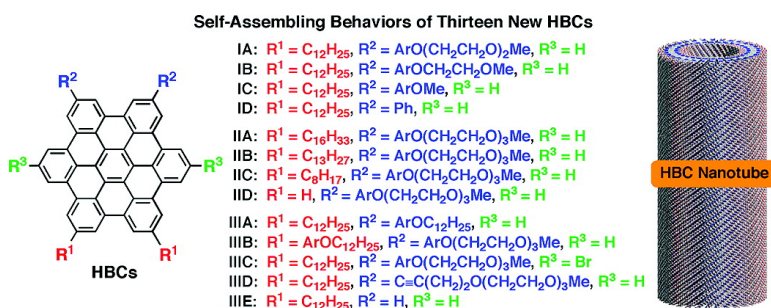Article

Systematic Studies on Structural Parameters for Nanotubular Assembly of Hexa-*peri*-hexabenzocoronenes

Wusong Jin, Yohei Yamamoto, Takanori Fukushima, Noriyuki Ishii, Jungeun Kim, Kenichi Kato, Masaki Takata, and Takuzo Aida

Self-Assembling Behaviors of Thirteen New HBCs

IA: $R^1 = C_{12}H_{25}$, $R^2 = ArO(CH_2CH_2O)_2Me$, $R^3 = H$
IB: $R^1 = C_{12}H_{25}$, $R^2 = ArOCH_2CH_2OMe$, $R^3 = H$
IC: $R^1 = C_{12}H_{25}$, $R^2 = ArOMe$, $R^3 = H$
ID: $R^1 = C_{12}H_{25}$, $R^2 = Ph$, $R^3 = H$
IIA: $R^1 = C_{16}H_{33}$, $R^2 = ArO(CH_2CH_2O)_3Me$, $R^3 = H$
IIB: $R^1 = C_{13}H_{27}$, $R^2 = ArO(CH_2CH_2O)_3Me$, $R^3 = H$
IIC: $R^1 = C_8H_{17}$, $R^2 = ArO(CH_2CH_2O)_3Me$, $R^3 = H$
IID: $R^1 = H$, $R^2 = ArO(CH_2CH_2O)_3Me$, $R^3 = H$
IIIA: $R^1 = C_{12}H_{25}$, $R^2 = ArOC_{12}H_{25}$, $R^3 = H$
IIIB: $R^1 = ArOC_{12}H_{25}$, $R^2 = ArO(CH_2CH_2O)_3Me$, $R^3 = H$
IIIC: $R^1 = C_{12}H_{25}$, $R^2 = ArO(CH_2CH_2O)_3Me$, $R^3 = Br$
IIID: $R^1 = C_{12}H_{25}$, $R^2 = C\equiv C(CH_2)_2O(CH_2CH_2O)_3Me$, $R^3 = H$
IIIE: $R^1 = C_{12}H_{25}$, $R^2 = H$, $R^3 = H$

HBCs

HBC Nanotube

More About This Article

Additional resources and features associated with this article are available within the HTML version:

- Supporting Information
- Access to high resolution figures
- Links to articles and content related to this article
- Copyright permission to reproduce figures and/or text from this article

View the Full Text HTML

Systematic Studies on Structural Parameters for Nanotubular Assembly of Hexa-*peri*-hexabenzocoronenes

Wusong Jin,*,[†] Yohei Yamamoto,[†] Takanori Fukushima,*,[$,†,‡] Noriyuki Ishii,[§]
Jungeun Kim,[#] Kenichi Kato,[⊥] Masaki Takata,[#,⊥,∥] and Takuzo Aida*,[†,‡]

ERATO-SORST Nanospace Project, Japan Science and Technology Agency (JST), National Museum of Emerging Science and Innovation, 2-41 Aomi, Koto-ku, Tokyo 135-0064, Japan, Department of Chemistry and Biotechnology, School of Engineering, and Center for NanoBio Integration, The University of Tokyo, 7-3-1 Hongo, Bunkyo-ku, Tokyo 113-8656, Japan, Biological Information Research Center, National Institute of Advanced Industrial Science and Technology (AIST), Tsukuba Central-6, 1-1-1 Higashi, Tsukuba, Ibaraki 305-8566, Japan, Japan Synchrotron Radiation Research Institute, 1-1-1 Kouto, Sayo-cho, Sayo-gun, Hyogo 679-5198, Japan, RIKEN SPring-8 Center, 1-1-1 Kouto, Sayo-cho, Sayo-gun, Hyogo 679-5148, Japan, and Department of Advanced Materials Science, Graduate School of Frontier Sciences, The University of Tokyo, 5-1-5 Kashiwanoha, Kashiwa, Chiba 277-8561, Japan

Received February 16, 2008; E-mail: jin@nanospace.miraikan.jst.go.jp; fukushima@riken.jp; aida@macro.t.u-tokyo.ac.jp

Abstract: Thirteen different hexa-*peri*-hexabenzocoronenes (HBCs) **I**−**III** were newly synthesized, and their self-assembling behaviors were investigated. Taking into account also the reported behaviors of amphiphilic HBCs, some structural parameters of HBC essential for the tubular assembly were revealed. Points to highlight include (1) the importance of two phenyl groups attached to one side of the HBC unit, (2) essential roles of long paraffinic side chains on the other side of the phenyl groups, and (3) no necessity of hydrophilic oligo(ethylene glycol) side chains. The hierarchical nanotubular structure, rendered by virtue of a synchrotron radiation technique, was virtually identical to our previous proposal, where the nanotubes are composed of helically coiled bilayer tapes with a tilting angle of ∼45°. Each tape consists of π-stacked HBC units, where the inner and outer HBC layers are connected by interdigitation of paraffinic side chains. The coiled structure is most likely caused by a steric congestion of the phenyl groups attached to the HBC unit, whose tilting direction may determine the handedness of the helically chiral nanotube.

Introduction

Self-assembled nanostructures consisting of π-conjugated molecules have attracted increasing attention because of their potential for organic and supramolecular electronics.[1] Polycyclic aromatic hydrocarbons are often utilized as building blocks for these materials,[2] where flexible side chains are usually incorporated into a rigid aromatic core, so that incompatible segments are phase separated from one another at a molecular level to enhance the ordering of aromatic units responsible for charge-carrier transport.[3] Hexa-*peri*-hexabenzocoronene (HBC) is the one with a highly extended π-conjugated system. Pioneering works have been made by Müllen and co-workers on the synthesis and self-assembly of HBC derivatives with paraffinic side chains, affording discotic liquid crystals and nanofibers.[4] Meanwhile, we developed a new class of Gemini-shaped HBC derivatives such as **1a** and **1b** (Figure 1), which possess two hydrophobic dodecyl chains ($C_{12}H_{25}$) on one side of the HBC core and two hydrophilic triethylene glycol

(TEG) chains on the other. Noteworthy is that these amphiphilic HBC derivatives self-assemble in polar solvents such as THF to form several tens of micrometers long nanotubes with a uniform diameter of 20 nm and a wall thickness of 3 nm. The proposed structure of the nanotube consists of helically rolled-up bilayer tapes composed of π-stacked HBC units, where the inner and outer HBC

[†] ERATO-SORST Nanospace Project, JST.
[‡] Department of Chemistry and Biotechnology, The University of Tokyo.
[§] National Institute of Advanced Industrial Science and Technology (AIST).
[#] Japan Synchrotron Radiation Research Institute.
[⊥] RIKEN SPring-8 Center.
[∥] Department of Advanced Materials Science, The University of Tokyo.
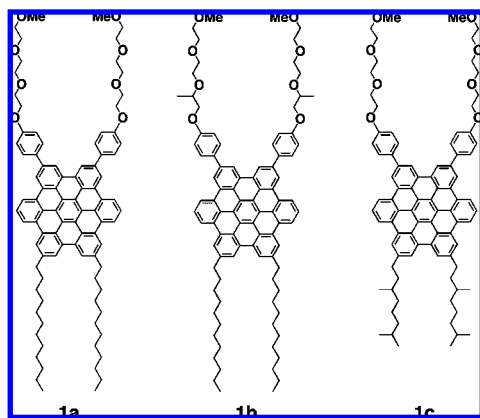[$] Present address: Advanced Science Institute, RIKEN, 2-1 Hirosawa, Wako, Saitama 351-0198, Japan.

(1) For recent reviews, see: (a) Lee, M.; Cho, B. K.; Zin, W.-C. *Chem. Rev.* **2001**, *101*, 3869–3892. (b) Carroll, R. L.; Gorman, C. B. *Angew. Chem., Int. Ed.* **2002**, *41*, 4378–4400. (c) *Molecular Electronics: Science and Technology*; Aviram, A., Ratner, M., Eds.; New York Academy of Sciences: New York, 1998. (d) Meijer, E. W.; Schenning, A. P. H. J. *Nature* **2002**, *419*, 353–354. (e) vander Auweraer, M.; de Schryver, F. C. *Nat. Mater.* **2004**, *3*, 507–508. (f) Hoeben, F. J. M.; Jonkheijm, P.; Meijer, E. W.; Schenning, A. P. H. J. *Chem. Rev.* **2005**, *105*, 1491–1546. (g) Schenning, A. P. H. J.; Meijer, E. W. *Chem. Commun.* **2005**, 3245–3258. (h) Grimsdale, A. C.; Wu, J.; Müllen, K. *Chem. Commun.* **2005**, 2197–2204. (i) Kumar, S. *Chem. Soc. Rev.* **2006**, *35*, 83–109. (j) Sergeyev, S.; Pisula, W.; Geerts, Y. H. *Chem. Soc. Rev.* **2007**, *36*, 1902–1929. (k) Wu, J.; Pisula, W.; Müllen, K. *Chem. Rev.* **2007**, *107*, 718–747. (l) Laschat, S.; Baro, A.; Steinke, N.; Giesselmann, F.; Hägele, C.; Scalia, G.; Judele, R.; Kapatsina, E.; Sauer, S.; Schreivogel, A.; Tosoni, M. *Angew. Chem., Int. Ed.* **2007**, *46*, 4832–4887. (m) de la Torre, G.; Claessens, C. G.; Torres, T. *Chem. Commun.* **2007**, 2000–2015. (n) Ajayaghosh, A.; Praveen, V. K. *Acc. Chem. Res.* **2007**, *40*, 644–656. (o) Ryu, J.-H.; Hong, D.-J.; Lee, M. *Chem. Commun.* **2008**, 1043–1054. (p) Thompson, B. C.; Fréchet, J. M. J. *Angew. Chem., Int. Ed.* **2008**, *47*, 58–77. (q) Goodby, J. W.; Saez, I. M.; Cowling, S. J.; Görtz, V.; Draper, M.; Hall, A. W.; Sia, S.; Cosquer, G.; Lee, S.-E.; Raynes, E. P. *Angew. Chem., Int. Ed.* **2008**, *47*, 2754–2787.

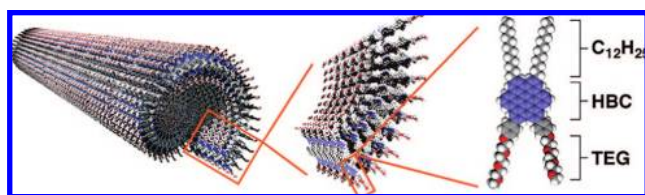**Figure 1.** Molecular structures of HBCs **1a**−**c**.

Figure 2. Schematic illustrations of the hierarchical structures of a nanotube formed from HBC **1a**.

layers are connected by interdigitation of the dodecyl side chains, while the TEG chains are located on both sides of the tubular wall (Figure 2). Namely, the tubular assembly appears to take place by an incompatibility between the hydrophobic and hydrophilic parts of the molecule. However, in some cases, we noticed that large hydrophobic groups incorporated into the TEG termini hardly hamper the nanotube formation. Examples include Gemini-shaped HBC amphiphiles with coumarin,[6] norbornene,[7] and trinitrofluo-

renone pendants[8] at one or both of the TEG termini. These observations prompted us to synthesize 13 different HBC derivatives (Figure 3) for rational understanding of the self-assembling process and also analyze the hierarchical nanotubular structure by means of wide-angle X-ray diffraction (WAXD) using a synchrotron radiation beam at SPring-8, BL02B2.

Results and Discussion

Synthesis of HBC Derivatives. The HBC derivatives in Figure 3 are classified into three categories. HBCs belonging to Group I all carry phenyl groups and dodecyl side chains. HBCs **IA** and **IB** possess at their phenyl groups oxyethylene side chains, which however are shorter than those of **1a**. While HBC **IC** carries methoxy groups instead of the oligoether side chains, **ID** possesses nonsubstituted phenyl groups. These compounds are designed to investigate possible roles of the hydrophilic oxyethylene side chains in the tubular assembly. HBCs in Group II all carry TEG chains, while their hydrophobic part bears paraffinic side chains of different lengths or nothing on an extreme of this series. They are intended to investigate effects of the paraffinic side chains on the tubular assembly. On the other hand, HBC derivatives in Group III are miscellaneous.

As described in detail in Supporting Information, HBC derivatives **IA** and **IB** were prepared by alkylation of **3** with tosylated derivatives of the corresponding oligo(ethylene glycol) monomethyl ethers, followed by oxidative cyclization of the resulting hexaarylbenzenes with $FeCl_3$ in $CH_2Cl_2/MeNO_2$ (Scheme 1).[9] A similar oxidation of **2** yielded **IC**.[9] For the synthesis of HBC derivatives **IIA**−**C** (Scheme 2), compound **5** with two bromophenyl groups was subjected to a Pd^{II}-catalyzed coupling reaction with the corresponding alkylmagnesium bromides to give hexaarylbenzenes **6a**−**6c**.[9] After the cleavage of their methoxy groups with BBr_3, the phenolic hydroxyl groups of the resulting hexaarylbenzenes were alkylated with 2-[2-(2-methoxyethoxy)ethoxy]ethoxy *p*-tosylate, affording hexaarylbenzenes **8a**−**8c**. Then, they were converted into HBCs **IIA**−**C** by oxidation with $FeCl_3$. HBC derivatives **IID**, **IIIA**−**C**, and **IIIE** were prepared from the corresponding diphenylacetylene and cyclopentadienone derivatives by a two-step synthetic protocol involving the Diels−Alder reaction and subsequent oxidation with $FeCl_3$.[9] For the synthesis of HBCs **ID** and **IIID**, dibrominated **IIIE** was likewise prepared from 4,4′-dibromodiphenylacetylene and didodecylcyclopentadienone and subjected to Pd^0-catalyzed coupling reactions with phenylboronic acid and TEG-appended acetylene, respectively.[9] All the HBC derivatives except **ID** were unambiguously characterized by NMR spectroscopy and MALDI-TOF mass spectrometry (Figure S1).[9] HBC **ID** showed an expected molecular ion peak in MALDI-TOF mass spectrometry but was hardly characterized by NMR spectroscopy because of its very poor solubility.

Self-Assembly of HBC Derivatives I. We investigated the self-assembly of HBCs **IA**−**C** under conditions identical to those optimized for **1a**. Typically, a THF suspension of **IA** with diethylene glycol side chains (1 mg/mL) was once heated at 50 °C, and the resulting yellow-colored solution was allowed to cool to 25 °C. A yellow suspension formed within a few hours. Electronic absorption spectroscopy of a cast film of the

(2) For reviews, see: (a) Harvey, R. G. *Polycyclic Aromatic Hydrocarbons*; Wiley-VCH: New York, 1997. (b) Randic, M. *Chem. Rev.* **2003**, *103*, 3449–3605. (c) *Carbon-Rich Compounds*; Haley, M. M.; Tykwinski, R. R., Eds.; Wiley-VCH, Verlag GmbH and Co., KGaA: Weinheim, 2006. (d) Anthony, J. E. *Angew. Chem., Int. Ed.* **2008**, *47*, 452–483.

(3) (a) van de Craats, A. M.; Warman, J. M.; Fechtenkötter, A.; Brand, J. D.; Harbison, M. A.; Müllen, K. *Adv. Mater.* **1999**, *11*, 1469–1472. (b) Schmidt-Mende, L.; Fechtenkötter, A.; Müllen, K.; Moons, E.; Friend, R. H.; MacKenzie, J. D. *Science* **2001**, *293*, 1119–1122. (c) Brédas, J.-L.; Beljonne, D.; Coropceanu, V.; Cornil, J. *Chem. Rev.* **2004**, *104*, 4971–5003. (d) Xiao, S.; Tang, J.; Beetz, T.; Guo, X.; Tremblay, N.; Siegrist, T.; Zhu, Y.; Steigerwald, M.; Nuckolls, C. *J. Am. Chem. Soc.* **2006**, *128*, 10700–10701.

(4) (a) Berresheim, A. J.; Müller, M.; Müllen, K. *Chem. Rev.* **1999**, *99*, 1747–1785. (b) Watson, M. D.; Fechtenkötter, A.; Müllen, K. *Chem. Rev.* **2001**, *101*, 1267–1300. (c) Rohr, U.; Kohl, C.; Müllen, K.; van de Craats, A. M.; Warman, J. *J. Mater. Chem.* **2001**, *11*, 1789–1799. (d) Simpson, C. D.; Wu, J.; Watson, M. D.; Müllen, K. *J. Mater. Chem.* **2004**, *14*, 494–504. (e) Wu, J.; Watson, M. D.; Zhang, L.; Wang, Z.; Müllen, K. *J. Am. Chem. Soc.* **2004**, *126*, 177–186. (f) Palermo, V.; Morelli, S.; Simpson, C.; Müllen, K.; Samori, P. *J. Mater. Chem.* **2006**, *16*, 266–271.

(5) (a) Hill, J. P.; Jin, W.; Kosaka, A.; Fukushima, T.; Ichihara, H.; Shimomura, T.; Ito, K.; Hashizume, T.; Ishii, N.; Aida, T. *Science* **2004**, *304*, 1481–1483. (b) Jin, W.; Fukushima, T.; Niki, M.; Kosaka, A.; Ishii, N.; Aida, T. *Proc. Natl. Acad. Sci. U.S.A.* **2005**, *102*, 10801–10806. (c) Yamamoto, Y.; Fukushima, T.; Jin, W.; Kosaka, A.; Hara, T.; Nakamura, T.; Saeki, A.; Seki, S.; Tagawa, S.; Aida, T. *Adv. Mater.* **2006**, *18*, 1297–1300.

(6) Motoyanagi, J.; Fukushima, T.; Ishii, N.; Aida, T. *J. Am. Chem. Soc.* **2006**, *128*, 4220–4221.

(7) Yamamoto, Y.; Fukushima, T.; Yamamoto, Y.; Kosaka, A.; Jin, W.; Ishii, N.; Aida, T. *J. Am. Chem. Soc.* **2006**, *128*, 14337–14340.

(8) (a) Yamamoto, Y.; Fukushima, T.; Suna, Y.; Ishii, N.; Saeki, A.; Seki, S.; Tagawa, S.; Taniguchi, M.; Kawai, T.; Aida, T. *Science* **2006**, *314*, 1761–1764. (b) Yamamoto, Y.; Fukushima, T.; N.; Saeki, A.; Seki, S.; Tagawa, S.; Ishii, N.; Aida, T. *J. Am. Chem. Soc.* **2007**, *129*, 9276–9277.

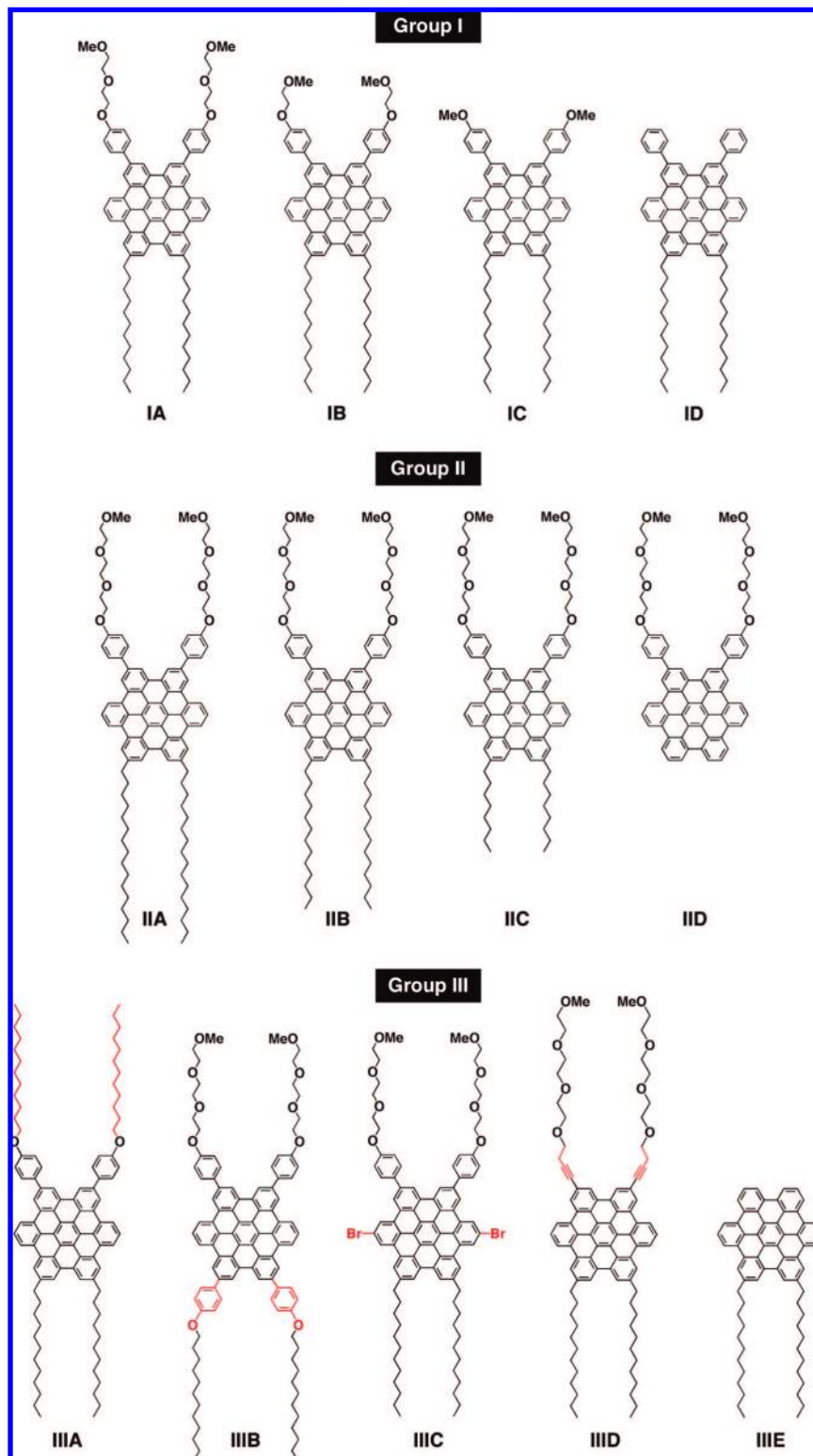(9) See Supporting Information.

Figure 3. Newly designed HBC derivatives **I**−**III**.

suspension displayed a main broadband at 366 nm with red-shifted absorption bands at 426 and 460 nm (Figure S2),[9] characteristic of tubularly assembled HBC units.[5−8] Scanning electron microscopy (SEM) of an air-dried suspension allowed for the visualization of cylindrical nano-objects with a hollow channel (Figure 4a). Transmission electron microscopy (TEM) showed that the nanotubes have a uniform diameter of 20 nm with a wall thickness of 3 nm (Figures 4b and 4c). Infrared

spectroscopy of the nanotubes cast on a KBr plate showed CH_2 stretching vibrations at 2918 (ν_{anti}) and 2849 (ν_{sym}) cm^{-1}, characteristic of paraffinic chains with a stretched conformation. Thus, it is most likely that the dodecyl chains interdigitate with one another to support a bilayer structure of the nanotube wall. All the above observations are analogous to those for the tubular assembly of **1a**. Moreover, a water droplet on a cast film of the nanotubes of **IA** showed a contact angle of 52.7 °, which is

Scheme 1. Synthesis of Gemini-Shaped HBC Derivatives **IA**–**C**[a]
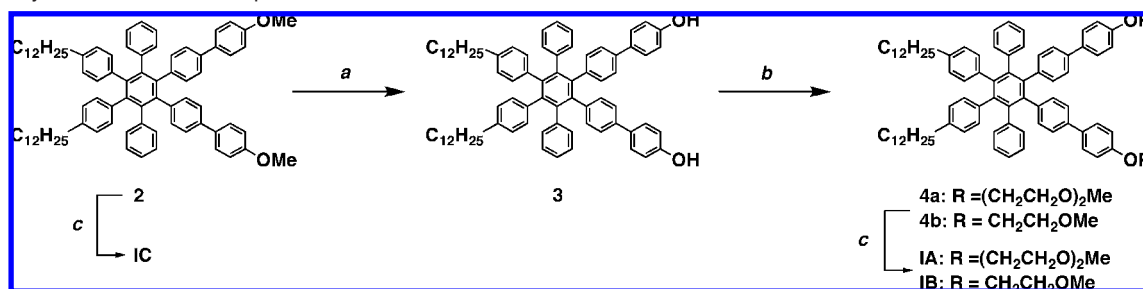
[a] Reagents and conditions: (a) BBr_3, CH_2Cl_2, 25 °C; (b) $TsO(CH_2CH_2O)_2Me$ or $TsOCH_2CH_2OMe$, KOH, THF, reflux; (c) $FeCl_3$, $MeNO_2$, CH_2Cl_2, 25 °C.

Scheme 2. Synthesis of Gemini-Shaped HBC Derivatives **IIA**–**C**[a]
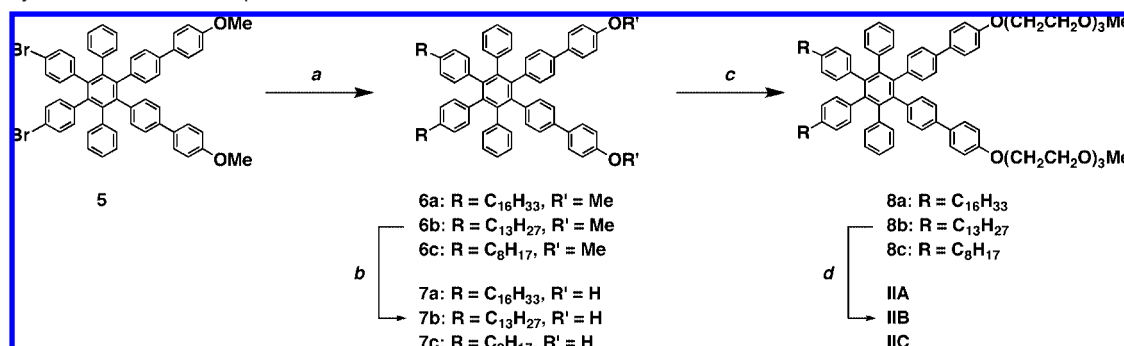
[a] (a) $C_{16}H_{33}MgBr$, $C_{13}H_{27}MgBr$, or $C_8H_{17}MgBr$, $PdCl_2(dppf)$, THF, reflux; (b) BBr_3, CH_2Cl_2, 25 °C; (c) $TsO(CH_2CH_2O)_3Me$, KOH, THF, reflux; (d) $FeCl_3$, $MeNO_2$, CH_2Cl_2, 25 °C.

comparable to that in the case of tubularly assembled **1a** (45.5 °) reported previously.[5a]

Similar to **1a** and **IA**, less hydrophilic **IB** carrying short ethylene glycol chains forms a nanotubular assembly (Figures 4d–f). However, to our surprise, even in the absence of ethylene glycol chains (**IC**), controlled self-assembly to give nanotubes took place (Figures 4g–i). Hence, one may conclude that the amphiphilic molecular design is not essential for the nanotubular assembly. Nevertheless, we noticed that the nanotubes of **IB** and **IC** (Figures 4d and 4g, respectively) are much shorter than that of **IA** (Figure 4a). Since **IB** and **IC** are less soluble than **IA** in THF, the corresponding nanotubular assemblies tend to precipitate out of the solution in a relatively early stage and lose the opportunity to grow further. Controlled self-assembly of **IA**–**C** also took place in CH_2Cl_2, a better solvent than THF, where the resulting nanotubes appeared to be longer than those formed in THF (Figure S3).[9] Unfortunately, self-assembling properties of **ID** were hard to investigate due to its extremely poor solubility.

Self-Assembly of HBC Derivatives II. In contrast with the HBC derivatives in Group I, those in Group II showed much different self-assembling behaviors from one another. For example, when a hot THF solution of **IIC** with octyl side chains (1 mg/mL) was allowed to cool to 25 °C, a yellow suspension resulted. However, TEM microscopy of an air-dried suspension displayed ill-defined aggregates (Figure 5c), with only a small amount of tubular and coiled assemblies. We also noticed that the electronic absorption bands above 400 nm, informative of the π-stacking manner of HBC, are quite obscure (Figure S2).[9] Furthermore, infrared spectroscopy showed CH_2 stretching vibrations at a higher wavenumber region (2923, 2852 cm^{-1}) than that observed for the dodecyl side chains in the tubular assembly of **1a**. As described in the above section and also reported in our previous papers,[5–8] the dodecyl side chains in

the tubularly assembled HBCs adopt a stretched conformation and interdigitate with one another to form a crystalline domain that supports the bilayer structure of the tubular wall. The essential role of the paraffinic side chains in the tubular assembly has also been suggested by the failure of the formation of nanotubes from **1c** (Figure 1) carrying branched paraffinic side chains incapable of crystallization.[5b] Thus, the octyl side chains of **IIC** are not long enough to form a crystalline domain important for the tubular assembly. Accordingly, HBC **IID** with no paraffinic side chains did not form nanotubes (Figure 5d).

We then investigated the assembly of a HBC derivative with longer paraffinic side chains such as **IIA** in CH_2Cl_2 and found that it self-assembles in a controlled manner to give nanotubes with a high structural integrity (Figure 5a). In this case, the choice of the solvent for self-assembly was rather critical, because an attempted assembly in THF under conditions optimized for tubular assembly of **1a**[5a] resulted in only a mixture of nanotubes and ill-defined aggregates (Figure S4). Noteworthy is that the nanotubes formed in CH_2Cl_2, as observed by TEM microscopy (Figure 5a), have the largest wall thickness (3.5 nm) and diameter (25 nm) among those obtained from HBC derivatives examined. The different size regimes, thus observed for the nanotubular assembly of **IIA**, seem likely, considering that the nanotube wall is supported by interdigitation of the paraffinic side chains. Namely, longer side chains upon interdigitation could result in a thicker bilayer wall. When such a thicker tape rolls up, a smaller curvature, i.e., a larger tube diameter, may be preferred.

Just for curiosity, we synthesized HBC **IIB** carrying tridecyl side chains with a view to investigate odd–even effects of the paraffinic side chains on the assembly. Under conditions similar to those for **1a**,[5a] compound **IIB** formed nanotubes whose size regimes (Figure 5b) and spectral profiles (Figure S2)[9] were essentially identical to those of the nanotubular assembly of **1a**.
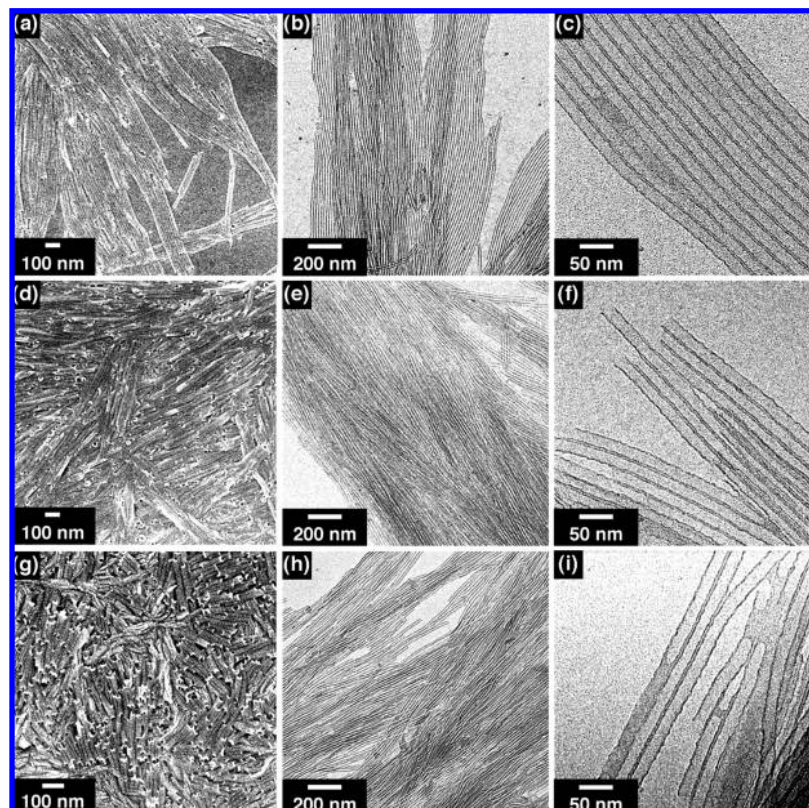
Figure 4. SEM and TEM micrographs of air-dried suspensions of **IA** (a−c), **IB** (d−f), and **IC** (g−i) assembled in THF.
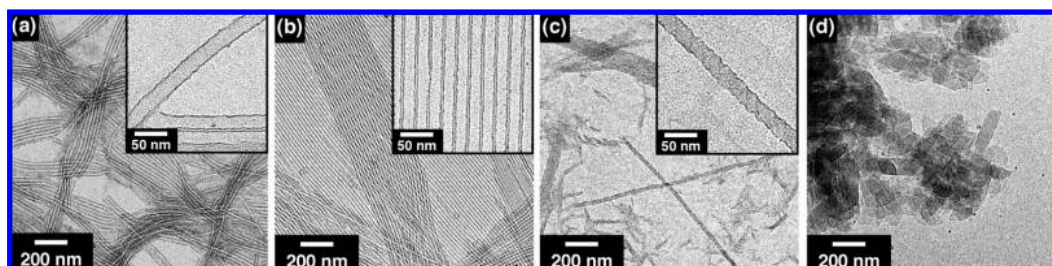

Figure 5. TEM micrographs of air-dried suspensions of (a) **IIA** assembled in CH_2Cl_2, and (b) **IIB**, (c) **IIC**, and (d) **IID** assembled in THF.

Self-Assembly of HBC Derivatives III. Groups III involves five different HBCs with much diverse structural variations. HBC **IIIA** carries dodecyl groups instead of the TEG chains in **1a**, while HBC **IIIB** involves a phenylene spacer for connecting the dodecyl side chains to the HBC unit. HBC **IIIC** is a dibrominated version of **1a** at the periphery of the HBC core. HBCs **IIID** and **IIIE** are essentially different from other HBC derivatives in that they do not bear phenyl groups. The former makes use of an alkyne functionality for anchoring the TEG chains to the HBC core, while the latter consists only of a HBC core and dodecyl side chains but does not possess TEG chains. In THF under the self-assembling conditions optimized for **1a**, none of these HBC derivatives formed nanotubes. Use of halogenated solvents such as CH_2Cl_2 and $CHCl_3$ instead of THF for the assembly again failed to form nanotubes. Moreover, we attempted vapor diffusion[5–8] using hexane or MeOH as a poor solvent in conjunction with THF or CH_2Cl_2, but no tubular objects resulted from HBC derivatives **III**. Figures 6a−e show typical TEM or SEM micrographs of the resultant aggregates. These nontubular assemblies did not exhibit red-shifted absorption bands (Figure S2).[9]

The most interesting result in the above experiments is certainly the unsuccessful nanotubular assembly of HBC **IIID** (Figure 6d), since it differs from **1a** only in the structure of the anchoring part for the TEG chains. In relation to this observation, Müllen and co-workers have reported the formation of nontubular filaments from amphiphilic HBC **9** (Chart 1) carrying imidazolium ion pendants.[10] Considering also the observation that **IIIE** did not form nanotubes but nontubular filaments (Figure 6e), we can conclude a crucial role of the phenyl groups in the controlled self-assembly to form a tubular morphology. Nevertheless, no nanotube formation from **IIIB** (Figure 6b) suggests that the phenyl groups should not be located on both sides of the HBC core. Thus, as can be seen in the HBCs belonging to Groups I and II, an ideal structural motif for the tubular assembly may involve two phenyl groups on the other

(10) Hamaoui, B. E.; Zhi, L.; Pisula, W.; Kolb, U.; Wu, J.; Müllen, K. *Chem. Commun.* **2007**, 2384–2386.

(11) Similar X-ray diffractions due to periodically aligned phenyl groups have been reported for a highly ordered one-dimensional assembly of a hexaaryl-HBC derivative. Pisula, W.; Tomovič, Ž.; Watson, M. D.; Müllen, K.; Kussmann, J.; Ochsenfeld, C.; Metzroth, T.; Gauss, J. *J. Phys. Chem. B* **2007**, *111*, 7481–7487.
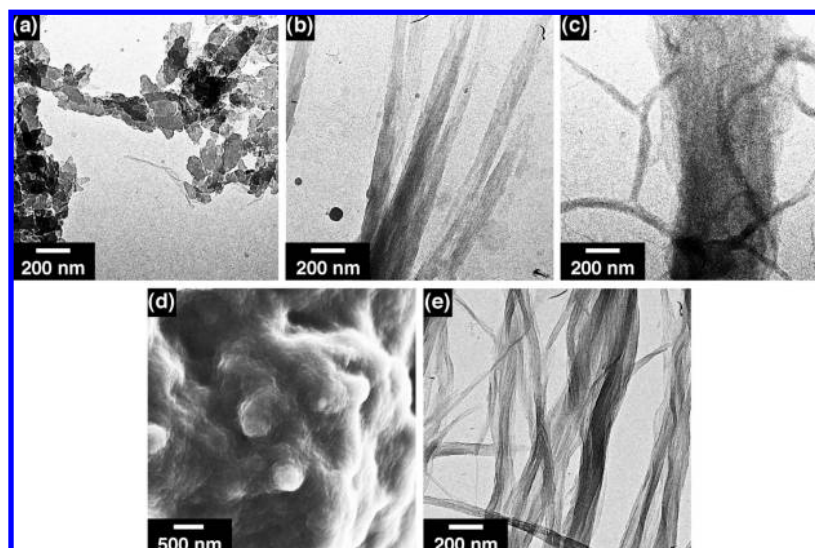
Figure 6. TEM micrographs of air-dried suspensions of (a) **IIIA** and (b) **IIIB** assembled in THF, (c) **IIIC** assembled in THF/MeOH (1:1 v/v), and (e) **IIIE** assembled in THF. (d) SEM micrograph of an air-dried suspension of **IIID** assembled in THF by MeOH vapor diffusion.

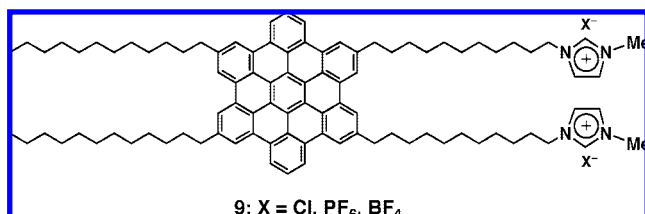**Chart 1.** Molecular Structure of HBC Derivative **9**[10]

Table 1. Structural and Spectral Characteristics of Tubularly Assembled HBC Derivatives

HBC	diameter (nm)[a]	d-spacing (nm)[b]	absorption maxima (nm)	C–H stretching (cm^{-1}) ν_{anti}	ν_{sym}
1a[c]	20	0.345	361, 429, 459	2918	2849
1b[d]	20	0.347	365, 398, 421	2917	2849
IA	20	0.344	366, 426, 460 (363, 426, 459)[e]	2918	2849
IB	20	0.345	364, 428, 458 (363, 429, 458)[e]	2918	2847
IC	21	0.345	367, 425, 462 (363, 431, 461)[e]	2917	2848
IIA	25	0.352	358, 428, 460[e]	2917	2848
IIB	20	0.347	359, 430, 460	2919	2849

[a] Determined by TEM microscopy. [b] Assigned to the cofacial HBC–HBC distance. [c] From ref 5a. [d] From ref 5b. [e] For the nanotubes formed in CH$_2$Cl$_2$.

side of the paraffinic side chains. However, the unsuccessful nanotube formation from **IIIA** (Figure 6a) suggests that the paraffinic side chains should be located only on one side of the HBC core. This configuration is certainly important for the selective formation of a bilayer tape without forming multilamellar structures. Finally, the failure of the nanotubular assembly of **IIIC** (Figure 6c), a dibrominated version of **1a**, is not surprising. As described in the following section, the nanotubular morphology is constructed from bilaterally connected columnar arrays of π-stacked HBC units, and such a bilateral connection can be hampered by bulky side groups of the HBC core.

Structural Aspects of Self-Assembled Nanotubes. Table 1 summarizes the spectral data of the self-assembled nanotubes obtained in this and previous studies.[5a,b] As already described, typical absorption spectral features include two red-shifted bands

characteristic of *J*-aggregates of π-stacked HBC units (Figure S2). Furthermore, infrared spectral characteristics include antisymmetric and symmetric stretching vibrations of the long alkyl side chains at 2917 (ν_{anti}) and 2848 (ν_{sym}) cm^{-1}, characteristic of a stretched conformation of paraffins on interdigitation. Furthermore, powder-pattern WAXD profiles of all the nanotubular assemblies are roughly identical to one another (Figures S5a),[9] except for the case of HBC **IIA** having longer hexadecyl side chains, where the *d*-spacing observed for the resulting larger-diameter nanotubes (*vide ante*) was slightly greater than those of the other cases. Apparently, the diffraction patterns of nontubular assemblies of **IIC**, **IID**, and **IIIE** (Figures S5b) were quite different from those of the nanotubular assemblies.

Having these features in mind, we conducted WAXD analysis of the nanotubular assembly of **1b** using a synchrotron radiation X-ray beam.[9] The nanotubes of **1b** have a great advantage, since they can be aligned unidirectionally into a macroscopic fiber,[5c] thereby making the diffraction pattern informative of the orientation of the π-stacked HBC units. Thus, a hot 2-MeTHF solution (50 °C) of (*S*)-**1b** (1.5 mg/mL) was allowed to cool to 25 °C, and the resultant suspension was aged for three weeks. Then, a glass hook was dipped into this suspension to collect the nanotube bundles and pulled up to stretch the captured aggregate to form a macroscopic fiber. By way of this simple macroscopic treatment, most of the nanotubes are aligned unidirectionally along the longer axis of the fiber.[5c] As shown in Figure 7a, we successfully obtained a two-dimensional (2D) WAXD image with a qualified diffraction pattern. At a *β*-angle (azimuthal angle from the longer-axis direction of the fiber) of 0°, a strong diffraction arc with a *d*-spacing of 0.347 nm was observed (Figure 7), indicating that the HBC units are π-stacked on top of each other and oriented perpendicular to the longer axis of the macroscopic fiber. Other characteristic diffraction arcs were observed at *β*-angles of approximately ± 45 and ± 27°, where the *d*-spacings for the former were ~0.48 and 1.03 nm, while that for the latter was 0.416 nm. Because of the longitudinal orientation of the nanotubes in the fiber, the diffraction feature of the fiber allows for elucidating the packing diagram of the assembled HBC molecules. As illustrated in Figure 8, the π-stacked columnar arrays of the HBC molecules are helically stranded (Figure 8b), where the central axes of these helical HBC columns are tilted by 45° relative to the longer axis of the tube (Figure 8c).
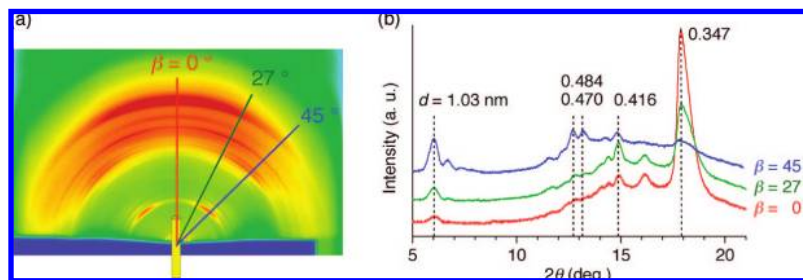
Figure 7. (a) 2D-WAXD image of a macroscopic fiber (4 mm in length and 0.2 mm in diameter) composed of the nanotubes of **1b** oriented unidirectionally along the longer axis of the fiber. (b) X-ray diffraction profiles of the fiber at β-angles of 0 (red), 27 (green), and 45° (blue).
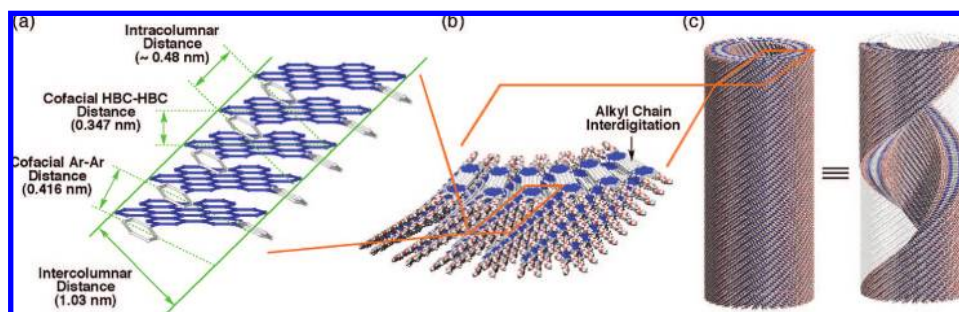

Figure 8. Schematic representations of the hierarchical self-assembled structures of HBC derivative **1b**. (a) π-Stacked columnar array, (b) bilayer wall, and (c) nanotube.

The d-spacing of 1.03 nm at $\beta = \pm 45°$ corresponds to the intercolumnar distance (Figure 8a). In each helical column, the HBC molecules stack up one another with an offset geometry. The d-spacings of 0.347 nm at $\beta = 0°$ and ~0.48 nm at $\beta = \pm 45°$ are assigned to the cofacial and center-to-center distances between the π-stacked HBC units (Figure 8a). Apparently, the offset helical geometry of the π-stacked HBC units allows the attached phenyl groups to be released from their possible steric congestion. For an energetic reason, the phenyl groups under such chiral environments might better tilt in either clockwise or counterclockwise direction relative to the HBC disk. In this context, the diffraction peak with a d-spacing of 0.416 nm at $\beta = \pm 27°$ is noteworthy. We assume that the phenyl groups may adopt a cofacial orientation with a tilting angle of 27° relative to the longer axis of the nanotube (Figure 8a).[11] Thus, the direction of this orientation may determine the handedness of the helical chirality of the nanotube.[5b]

Conclusions

Through the systematic investigation of the self-assembling behaviors of 13 new Gemini-shaped hexa-*peri*-hexabenzocoronene (HBC) derivatives **I−III**, some structural parameters essential for the nanotubular assembly were revealed. Although we have often emphasized the importance of amphiphilic molecular design for the nanotube formation,[5−8] the real essence of this design turned out to be for making this discotic π-conjugated molecule less symmetrical by incorporating two phenyl groups and paraffinic side chains on opposite sides. This is quite encouraging, since one may take more advantage of such a design flexibility for structural elaboration and functionalization of the nanotubular assembly. Also noteworthy is the

first and nearly perfect structural elucidation of the HBC nanotube, using a synchrotron radiation technique. The diffraction pattern of the nanotube of **1b** successfully rendered the hierarchical structure composed of a number of bilayers laterally coupled and grown helically (Figure 8). Through these studies, we now recognized that our adventitious molecular design for the prototype HBC amphiphile includes a variety of tricks that lead to the nanotubular assembly. Most important may be the presence of two phenyl groups on one side of the HBC unit, which allows the molecule to π-stack on top of each other in an offset, helical geometry. Although triethylene glycol (TEG) chains in the prototype molecular design are not essential, they help the resultant nanotubes stay as long as possible in solution and grow up to a macroscopic dimension. Furthermore, the flexible TEG chains can make the nanotube formation virtually intact to their terminal functionalities, usable for surface-functionalization of the nanotubes.

Supporting Information Available: Details of synthesis and characterization of HBC derivatives **I−III**, MALDI-TOF mass and electronic absorption spectra, TEM micrographs, and X-ray diffraction patterns. This material is available free of charge via the Internet at http://pubs.acs.org.

JA801179E